Scintimetric Evaluation of Remodeling after Bone Fractures in Man

Jörg Spitz, Isabelle Lauer, Klaus Tittel and Hanfried Weigand

Departments of Nuclear Medicine and Central X-ray, Municipal Hospital, Wiesbaden; and Evangelisches Krankenhaus Oldenburg, Germany

In a review of bone scans of 2000 post-trauma patients, the following rules of bone remodeling after fracture were found: different bones behave differently; lesions in the vicinity of joints show an early and high accumulation of the tracer within the first days after the trauma, whereas fractures of the axial skeleton and shafts of long bones sometimes need up to 12 days to appear on scan; all except skull fractures demonstrate a steady rise of accumulation intensity compared to normal bone for 2–5 wk; the steepness of increase and time of maximum differ significantly for different fracture sites. Calculating a ratio 24:4 hours after injection helps differentiate fractures from soft tissue lesions since fresh fractures show a ratio >1.1. We found no clinically relevant dependence on sex and age. The scintigraphic/scintimetric behavior of fractures is reproducible and predictable, adding specificity to the well-known high sensitivity of bone scans.

J Nucl Med 1993; 34:1403–1409

Since Subramanian (*1*) described the ^{99m}Tc-labeling of phosphate compounds in 1971, bone scintigraphy has become one of the most important routine nuclear medicine procedures. Initially, oncological indications predominated, however orthopedic and traumatic questions soon grew in importance. Although there is ample literature addressing bone scintigraphy, trauma and orthopedics (*2–6*), there is minimal quantitative data regarding bone remodeling after trauma.

We retrospectively screened over 2000 patients who underwent bone scintigraphy after trauma. Results indicate that scintimetric evaluation of bone remodeling after trauma adds specificity to the high sensitivity of bone scanning.

MATERIAL AND METHODS

Of 2000 cases, only those with complete clinical data and a final diagnosis were selected. More than two-thirds (1369) showed at least one fresh fracture documented by x-ray and CT. One-third of these had their scintigraphic data archived on floppy or optical disk, allowing retrospective semiquantitative evaluation (scintimetry).

Twenty-Four-Hour Scintimetry

In addition to retrospective evaluation, we prospectively investigated some trauma patients with a special protocol. Formal consent was given by 18 patients (10 women, 8 men) to be investigated several times up to 24 hr after injection. Patient age ranged from 27–73 yr. Three patients had two bone lesions.

Scintimetry of Different Fracture Sites up to 100 Days After Trauma

Fractures in 480 patients were investigated: 123 thoracic and lumbar spine, 100 distal radius, 101 os scaphoid, 59 femoral neck, 48 pelvis and 49 shafts of long bones of the extremities. Of the shaft fractures, 68% where treated surgically by fixation with metal plates, whereas only 10% in the distal radius where surgically treated. Fractures of the spine, the os scaphoid and the pelvis where treated conservatively in almost 100% of cases.

Except for the group with fractures of the os scaphoid (6 women and 26 men), sex distribution was equal in all groups. Age ranged from 6 to 88 yr (mean value: 46 yr).

Methods

All patients where investigated with ^{99m}Tc-HMDP (CIS International) on a digital gamma camera (APEX-415, Elscint) with a low-energy, general purpose collimator. The individual dose of ^{99m}Tc-HMDP was 7–10 MBq/kg body weight for adults and 4 MBq/kg body weight for children.

In the group with 24-hr scintimetry, the first scintigrams were done 5-min after injection, then at 2-hr, 4-hr, 6-hr and 24-hr intervals. Only in seven of 18 patients could the protocol be completed for 10 lesions. Six lesions (in four patients) were qualified as new fractures (10–18 days after trauma) and four (in three patients) as soft-tissue lesions or degenerative changes.

Investigation time for the large patient group with different fracture locations ranged from 2 hr to 6 hr after injection. The mean investigation time was 3.3 hr. All scintigrams were stored in 16k matrices (128 × 128 pixels) on floppy or optical disc. Quantitative evaluation of data (scintimetry) was done by applying known routine procedures to the planar images (*7*): rectangular, irregular or circular regions of interest (ROI) were drawn around the fracture site and a reference region, either on the contralateral site of the body or, in case of the spine, around the next, noninvolved vertebral body above and below fracture. The bone remodeling ratios were calculated by dividing the number of counts per pixel at the fracture site by the number of counts per pixel in the reference area.

In addition to these general ratios, data of patients with 24-hr

Received Mar. 26, 1992; revision accepted Sept. 21, 1992.

For correspondence and reprints contact: Priv.-Doz. Dr. J. Spitz, RNS Wiesbaden (Nuklearmedizin) Städt. Klinikum, Ludwig-Erhard-Str. 100, 65199 Wiesbaden, Germany.

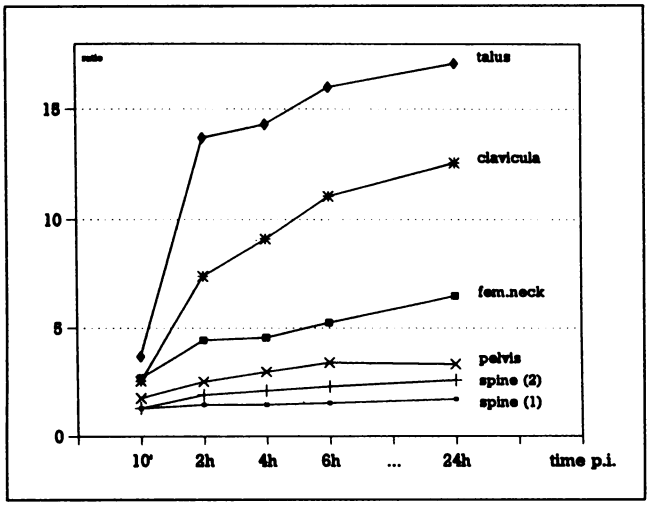

FIGURE 1. Twenty-four-hour scintimetry of different fresh fractures (ratio of the accumulation intensity at fracture site compared to a normal reference site).

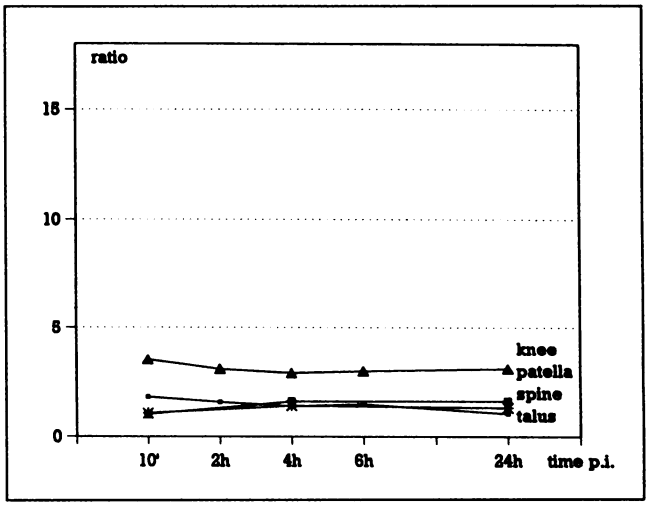

FIGURE 2. Twenty-four-hour scintimetry of degenerative processes (ratio of accumulation intensity at the lesion compared to a normal reference site).

scintimetry were evaluated by calculating a 4:24-hour ratio at the site of the bone lesion (*8*).

To evaluate the reproducibility of scintimetry, calculations of various ROIs with different sizes and shapes were performed 10 times, calculating the coefficient of variation. Further, the influence of a plaster cast on scintimetry was studied by measuring the absorption of a wedge-shaped plaster cast of 1–50 mm thickness, positioned on a field flood source.

Statistical analysis was done with a SAS software package by Prof. Hommel from the department of medical statistics and documentation of the Johannes-Gutenberg-University in Mainz, FRG.

RESULTS

Technical Aspects

Variations of less than 5% were found when the same operator used regular and irregular ROIs to calculate 10 times the accumulation intensity of fractures of the distal radius, os scaphoid and lumbar spine, compared to the corresponding normal site. Larger reference ROIs gave lower variations. A flood field with ^{99m}Tc showed an absorption of about 10% per 10 mm thickness of a wedge-shaped plaster cast. A bar-phantom interposed between the flood field and the wedge showed no interference with resolution of the 6 mm bars up to 5 cm plaster thickness.

Twenty-Four-Hour Scintimetry

All fresh fractures showed increasing accumulation at the fracture site during 24 hr after injection. But the magnitude of increase differed markedly by site (Fig. 1). Comparing accumulation intensity after 24 hr to accumulation intensity after 4 hr of the same fracture resulted in a ratio higher than 1.1 in each case. In contrast, soft-tissue lesions and degenerative processes showed lower ratios and no relevant increase of accumulation intensity within 24 hr (Fig. 2).

Scintimetry of Different Fracture Sites at Intervals after Trauma

Scintimetric evaluation of the 480 fracture sites resulted in typical behavior, showing rising ratios within the first 2–3 wk after trauma. However, in the first days, different bones behaved in different ways: fractures near the joints of the distal upper and lower extremities showed ratios higher than 2.0 already on the day of the trauma. Fractures of the spine and pelvis showed ratios equal to 1.0 or between 1 and 1.5 within the first days. Fractures of the femoral neck behaved similarly with ratios that did not exceed 2.0 for the same time period. For example, Figure 3 shows the calculated ratios of pelvic, distal radius and spinal fractures within 3 wk after trauma.

Compared to fractures of the spine, fractures of the distal radius clearly show higher mean values within the first days post-trauma and also at the time of maximal accumulation 2–3 wk after trauma. The mean ratios for all

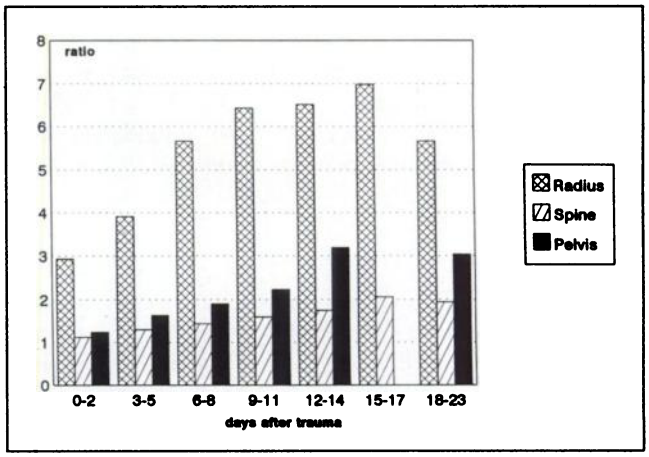

FIGURE 3. Mean ratios of individual fractures of the pelvis, spine and distal radius for three-day periods (last group = 6-day period). Missing values for fractures of the pelvis between day 15 and 17.

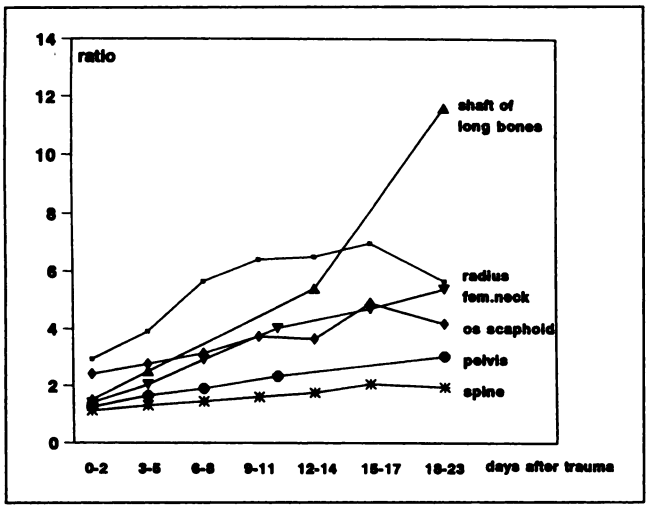

FIGURE 4. Different scintimetric behavior of fractures at different fracture sites (fracture-to-normal reference site).

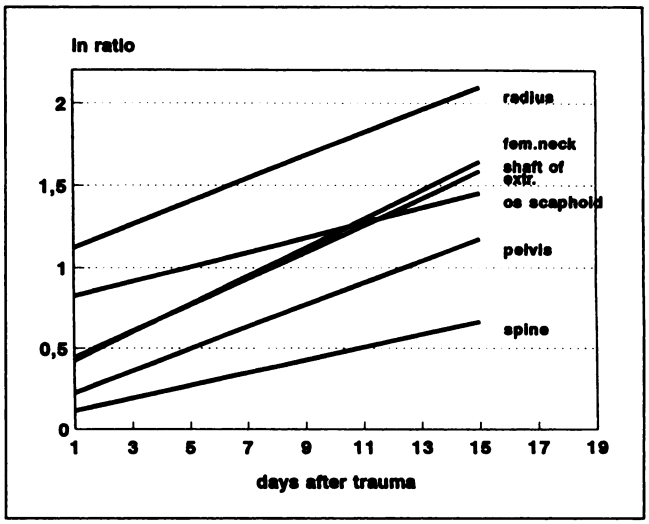

FIGURE 5. Linear regression curves of the ratios (ln) of different fracture sites (fracture-to-normal reference site).

fracture locations are compared in Figure 4. The differing behavior of lesions in different bones is obvious.

STATISTICAL ANALYSIS

To evaluate the visual observations of Figure 4 we applied different statistical tests to the results.

T-Test After Bonferroni-Correction

In a first step, the mean values of the time periods for different fracture sites were compared by the Students t-Test after Bonferroni-correction to observe whether calculated differences of the time intervals are significant (Table 1).

Linear Regression Analysis

After transformation of values of each fracture location in their natural logarithm, a linear regression analysis was done for the first 15 days:

$$\ln(q) = a + b \times t,$$

where a represents the intercept, b is the slope and t is the time after the trauma.

Linear regression curves were different for all bones but always were positive (Fig. 5). All intercepts were different from 0. However fractures of the axial skeleton and shafts of long bones showed smaller intercepts than lesions in the proximity of joints.

Multiple Linear Regression Analysis

Slopes and intercepts of regression equations where submitted to the following regression model:

$$\ln(q) = a + b1 \times t + b2 \times m + b3 \times m \times t,$$

TABLE 1
Significance of Ratios (t-test after Bonferroni correction)

	Days						
	0–2	3–5	6–8	9–11	12–14	15–17	18–23
Site 1–2	t	B	B	B	t	ns	ns
Site 1–3	B	B	B	t	t	ns	ns
Site 1–4	B	B	B	B	B	B	B
Site 1–5	B	B	B	B	ns	—	B
Site 2–3	B	t	ns	ns	ns	ns	ns
Site 2–4	B	B	B	B	B	B	B
Site 2–5	B	B	B	B	ns	—	ns
Site 3–4	ns	B	B	B	ns	B	B
Site 3–5	ns	ns	B	B	ns	—	t
Site 4–5	ns	ns	t	t	ns	—	t
Site 6–1	B	B	B	B	ns	—	ns
Site 6–2	t	t	ns	ns	ns	—	B
Site 6–3	ns	ns	ns	t	ns	—	ns
Site 6–4	ns	B	B	B	B	—	B
Site 6–5	ns	t	t	t	ns	ns	—

ns = differences not significant; t = differences significant in Student-t-test; B = differences significant in t-test after Bonferroni correction; — = no ratios for this subgroup.
site 1 = distal radius; site 2 = os scaphoid; site 3 = femoral neck; site 4 = spine; site 5 = pelvis; site 6 = shaft of extremities.
Significance level 5%.

TABLE 2
Significance of the Differences of Intercepts and Slopes

	Difference intercept	p intercept	Difference slope	p slope
Site 1–2	−0.276	0.0081	−0.024	0.0777
Site 1–3	−0.718	0.0001	0.018	0.3164
Site 1–4	−0.975	0.0001	−0.031	0.0001
Site 1–5	−0.897	0.0001	−0.002	0.9175
Site 2–3	−0.413	0.0040	0.037	0.0188
Site 2–4	−0.699	0.0001	−0.006	0.4874
Site 2–5	−0.621	0.0001	0.023	0.0085
Site 3–4	−0.257	0.0010	0.049	0.0001
Site 3–5	−0.099	0.4916	−0.034	0.0351
Site 4–5	0.078	0.2435	0.029	0.0023
Site 6–1	−0.694	0.0001	0.012	0.5309
Site 6–2	−0.418	0.0209	0.036	0.0828
Site 6–3	0.024	0.9185	−0.006	0.8232
Site 6–4	0.281	0.0093	0.043	0.0004
Site 6–5	0.203	0.3400	0.014	−0.6141

Significance level $p < 5\%$.
Site 1 = distal radius; site 2 = os scaphoid; site 3 = femoral neck; site 4 = spine; site 5 = pelvis; site 6 = shaft of extremities.

where q = ratio [fracture to normal site], t = time after trauma, m = 0 for loc(i), m = 1 for loc(j). Each time only two locations (i.e., loc(i) and loc(j)) are compared. Statement for b_3: difference of the slopes, statement for b_2: difference of the intercepts.

Table 2 shows the results of statistical analysis for different fracture sites.

Squared Regression Analysis

To find the angular point corresponding to the time of the most intensive bone remodeling, ratios were analyzed with the following equation:

$$\ln(q) = a + b \times t + b_2 \times t^2.$$

The values ranged from 17.2 days for fractures of the distal radius to 35.1 days for fractures of long bones. The r^2 values ranged from 0.8 for fractures of the os scaphoid to 0.7 for fractures of the femoral neck.

Multiple Regression Analysis with Regard to the Age of the Patient

To estimate the influence of patient age on bone remodeling after a fracture, ratios of the spinal fractures were analyzed with the following equation:

$$\ln(q) = a + b1 \times t + b2 \times t^2 + b3 \times \text{age},$$

considering patient age as an additional factor besides the time after the trauma. The p-value for b3 (age) was found to be 0.05. The total r^2 of the equation was 0.69 and the r^2 for the factors (time after trauma) and (time after trauma)^2 was 0.68. Thus, for the factor b3 (age), a r^2 of 0.01 is left.

Mean Values of Different Age Groups

Ratios of all spinal fractures within the first three days after trauma were divided into age groups up to 55 yr (n = 17) and over 55 yr (n = 14). Mean values were 1.17 ± 0.13 versus 1.13 ± 0.12 (p = 0.38). Comparison of a second time interval (8–11 days) gave almost the same result with regard to significance: 1.51 versus 1.61 (p = 0.12).

Multiple Regression Analysis with Regard to Patient's Sex

Except for one-time subgroup of the spinal fractures, all p-values were >0.05, thus revealing no significant sex-related differences in bone remodeling after fracture.

DISCUSSION

Only five publications concerning bone scintimetry under clinical conditions were found in a review of the literature (*9–13*). All deal with one fracture location only: one article with the spine, two with the tibia and two with the distal radius. None compared bone remodeling at different fracture sites. The number of investigated cases also is much lower, except in spinal fractures (*10*). Although there are methodological differences, the trends of reported results largely agree with our data.

Some experimental work concerning quantitative data after fractures in animals exists (*6,14–20*). However, most of this work was done with the tibiae of rats and some with the tibiae of rabbits.

One publication reports on experimental fractures of the radius in baboons (*18*). The authors evaluated fracture healing of long bones in 11 animals after subjecting them to 44 controlled fractures of radius and ulna. In three-phase scintigraphy they found an early steep rise in activity accumulation due to reactive blood perfusion in the first days, maximum activity ratios at 21 days and thereafter a gradual decrease in activity at the fracture site. These data are in agreement with the scintimetric results of fractures of the distal radius in our patients.

Before initiating retrospective evaluation of clinical data, we checked the qualitative and quantitative influence of the plaster cast on scintigraphic/scintimetric results. Calcu-

lated absorption of 10%/cm plaster of the wedge is in agreement with the few reports in the literature (*9,21*) and allows scintigraphy and scintimetry without removing the plaster cast. The influence of the plaster with an absorption of 10%–20% is negligible compared to the biological variations and changes in accumulation intensity with ratios up to 500%–800%. The same is true with our coefficients of variation for repeated calculations on the basis of various ROIs, which are in good agreement with the literature (*11,15,21*).

Regarding clinical data, we found a continuous increase of ratios up to 24 hr after injection. Similar behavior has been observed in benign and malignant bone lesions. In 1975, Citrin (*22*) reported increasing activity in tumor lesions of the spine up to 4 hr after injection, while normal vertebrae remained at the same activity level after 2 hr. Ten years later, Israel and coworkers (*23*) calculated a 24:4 hr/activity ratio, which was significantly lower in patients with degenerative changes of the spine compared to vertebrae with untreated bone metastasis of breast or prostate cancer.

One year later, Castronovo (*24*) reported significantly increased 4-hr and 24-hr whole-body retention of ^{99m}Tc-MDP in patients with prostate cancer, compared to patients with osteoporosis. Alazraki (*25*) used 4-phase scintigraphy to distinguish between osteomyelitis and peripheral vascular disease by adding 24-hour static images to the 3-phase scintigraphy. Patients with osteomyelitis showed progressively increasing lesion-to-background activity ratios over time. In 1987, Israel and coworkers (*8*) used their experience with tumor lesions and adapted their 24:4-hr/activity ratio technique to distinguish osteomyelitis from soft-tissue infection.

Explanation for this behavior of benign and malignant lesions is given by Arnold (*26*), who developed a two-compartment model based on the fact that woven bone, which is produced around osteomyelitis and primary or metastatic bone tumors, contains large amounts of amorphous calcium phosphate. To this, ^{99m}Tc phosphate compounds are tightly bound, whereas to normal bone it is loosely bound and thus exchangeable. Uptake curves of the bone lesions demonstrate increasing amounts of the labeled phosphate compounds over time, while those of normal bone fall progressively during 4–24 hr.

Fresh fractures also contain large amounts of woven bone. It should then be expected that traumatic lesions would behave similarly to bone tumors and osteomyelitis.

Indeed, we found a continuous increase of the ratios up to 24 hr after injection, while the behavior of soft-tissue lesions and degenerative changes, resulting in either slowly decreasing or horizontal curves was identical to previous reports in the literature (*8,22–26*).

In addition, except for the first days after fracture, calculated ratios are usually much lower for soft-tissue lesions in comparison to fractures and rarely exceed a ratio of 3.0. This fits the concept that reactive hyperaemia will increase accumulation of ^{99m}Tc-MDP only by a factor of 2–3 (*27*).

Our 24-hr scintimetry data are not numerous enough to be validated statistically. However, since they are consistent with experimental and clinical data in the literature, it seems appropriate to observe that by comparing the 24-hr accumulation ratio to the 4-hr accumulation, ratios below 1.1 exclude a fresh fracture.

Within the first 2 wk, all fractures showed a continuous rise in calculated ratios. But we noticed significant differences concerning the initial intensity and steepness of the further rise of the accumulation intensity of different fracture sites. As a rule, fractures of the axial skeleton showed accumulation ratios only slightly higher than 1.0 compared to fractures in the proximity of joints with ratio higher than 2.0 in the first days after trauma.

Interpretation of these statistically significant differences is not easy, particularly as no animal experiments with fractured bones of the spine and pelvis exist. One reason for the difference might be the blood supply of the various bones. Rhinelander (*28,29*) demonstrated a significant delay in callus formation in tibial fractures, depending on whether or not the fracture was dislocated, since dislocation leads to a disruption of local bone blood supply. Huittinen and Slätis (*30*) report on postmortem observations of multiple-injury patients. They found an unexpectedly high incidence of fractures of the dorsal pelvic ring combined with disrupted vessels. As in the study of dislocated fractures of the tibia, interrupted blood supply could explain the slow reaction of the pelvic bone after fracture.

All fresh fractures typically showed rising ratios until they peaked between 2–5 wk post-trauma. There were significant differences in the steepness of the calculated slope of different bones. The reason for these differences is the extent of callus formation of different bones, which can be easily understood by comparing the large callus reaction of a femoral fracture treated by plaster cast to the small response of a broken vertebral body.

Fractures of the skull support this interpretation. In a study to be published elsewhere, we screened a large group of multiple-injury patients, five of whom had fractures of the skull. Only one showed a very faint accumulation in the bone scan, the other four showed no callus reaction at all. In another multiple-regression analysis we tried to support Matin's thesis (*31*) that appearance time of fractures depends on patient age. The multiple-regression analysis of spinal fractures showed, however, that age as factor added only 1% to interpretation of values, compared to 68% by the factor of time after trauma. Similarly, the mean values of different age groups showed no significant difference in bone remodeling between younger and older patients.

Despite different conclusions, Matin's data are consistent with the present: Matin considered only patient age and not the fracture site: 20 patients who were investigated within 24 hr after fracture showed positive reaction in 16 cases. Of four patients with negative reaction, three were older than 65 yr, leading to the conclusion that appearance time is age-dependent. However, two had a femoral neck fracture and one a compression fracture of the spine. The

fourth patient with negative reaction also showed a fracture of the spine, but was only 10 yr old. Thus, all four patients with negative reaction had fractures of the axial skeleton or shafts of long bones even though one was only 10 yr old.

Other publications support these findings and report delay in scintigraphic appearance time of fractures of the spine and pelvis (*32–35*).

SUMMARY

Synopsis of our scintimetric data and of clinical and experimental data of the literature leads to the following general rules of bone remodeling after fracture in humans:

1. Within 24 hr after fracture, the affected bone and its surrounding area may show diffuse reactive increase in perfusion.
2. The extent and intensity of initial accumulation depends on the fracture site. Lesions in the proximity of joints show up immediately, lesions of the axial skeleton and shafts of long bones sometimes only after 10–12 days.
3. In the subsequent 2–3 wk, all fresh fractures show an increasing accumulation of tracer. The scale of this increase in accumulation intensity is significantly different for the different fracture sites.
4. Similar bones at different skeletal sites (i.e., thoracic and lumbar spine or the shafts of humeri, femur and tibia) show similar behavior.
5. Depending on fracture site, the peak of tracer accumulation was found between 2–5 wk post-trauma.
6. Different fracture sites show different accumulation intensity after injection and different extent of increase in accumulation in the following 24 hr.
7. The calculation of a 24:4 hr ratio allows differentiation of a fracture from soft-tissue lesions with reactive hyperemia, the fractures showing values higher than 1.1.
8. Patients' age and sex have no clinical relevance for the extent of bone remodeling post-trauma.

ACKNOWLEDGMENT

The authors thank Ingrid Pfaff for expert technical assistance; Sigrid Schenk for secretarial assistance and skillful drawings; and Prof. Dr. Hommel, department of statistical analysis, J. Gutenberg University, Mainz. This work was presented in part at the 38th Annual Meeting of the Society of Nuclear Medicine, 1991.

REFERENCES

1. Subramanian G, McAfee JG. A new complex of Tc-99m for skeletal imaging. *Radiology* 1971;99:192–196.
2. Francis MD. Tc-99m-diphosphonate uptake mechanism on bone. In: Fogelman I, ed. *Bone scanning in clinical practice*. Springer Verlag: New York; 1987:7–17.
3. Galasko CSB, Weber DA. Radionuclide scintigraphy. In: *Orthopaedics (Current Problems In Orthopaedics)*, Edinburgh: Churchill Livingston; 1984.
4. Matin P. Bone scanning of trauma and benign conditions. In: Freeman LM, Weissmann HS, eds. *Nuclear medicine annual 1982*. New York: Raven Press; 1982;81–118.
5. Matin P. Bone scintigraphy in the diagnosis and management of traumatic injury. *Semin Nucl Med* 1983;13:104–122.
6. Rosenthall L, Lisbona R. Role of radionuclide imaging in benign bone and joint disease of orthopedic interest. In: Freeman LM, Weissman HS, eds. *Nuclear medicine annual 1980*, New York: Raven Press; 1980;267–301.
7. Smith ML. Quantitative Tc-99m diphosphonate uptake measurements. In: Fogelman I, ed. *Bone scanning in clinical practice*. New York: Springer Verlag; 1987;16:237–248.
8. Israel O, Gips S, Jerushalmi J, Frenkel A, Front D. Osteomyelitis and soft-tissue infection: differential diagnosis with 24 hour/4 hour ratio of Tc-99m MDP uptake. *Radiology* 1987;163:725–726.
9. Greiff J. The time course of Tc-99m-Sn-polyphosphate scintimetry of normally healing tibia fractures in man. *Injury* 1981;13:69–75.
10. Keyl W, Milachowski KA, Zwingers T. Die quantifizierende knochenszintigraphie in der beurteilung der wirbelkörperfraktur. *Hefte zur Unfallheilkunde* 1983;165:173–174.
11. Lund B, Lund JO, Sorensen OH, Lund B. Evaluation of fracture healing in man by serial Tc-99m-Sn-Pyrophosphate scintimetry. *Acta Orthop Scand* 1978;49:435–439.
12. Wahlström O. Studies of Colles' fracture. Dissertation, Linköping University No. 160, 1983.
13. Zechmann W, Oberhammer J. Szintigraphische verlaufskontrollen der frakturheilung bei unterschenkelfrakturen. *Zeitschrift für Allgemeinmedizin* 1976;27:1374–1377.
14. Hellerer O, Brückner WL, Aigner R, Westerburg KW, Kleinschmidt J. Modell zum studium von einflüssen auf die frakturheilung. tierexperimentelle untersuchungen. *Chir Forum Exp Klin Forsch* 1979:189–192.
15. Greiff J. Bone healing in rabbits after compression osteosynthesis, studied by Tc-99m(Sn)polyphosphate scintimetry and autoradiology. *J Nucl Med* 1981;22:693–698.
16. Becker W, Dreyer J, Georgi P. Wert der szintigraphie bei frakturen und pseudarthrosen. *Hefte zur Unfallheilkunde* 1974;117:242–246.
17. Klug W, Franke W-G, Schulze M. Tierexperimentelle szintigraphische verlaufskontrolle der frakturheilung. *NucCompact* 1983;14:217–223.
18. Mennen U, Dormehl IC, Goosen DJ, Grove HA. Evaluation of the healing process of bone fractures in the non-human primate using sequential Tc-99m-methylene diphosphonate scintigraphy. *South African Journal of Surgery* 1985;23:98–101.
19. Bushberg JT, Hoffer PB, Schreiber GJ, Lawson AJ, Lawson JP, Lord P. Comparative uptake of Ga-67 and Tc-99m MDP in rabbits with a benign noninfected bone lesion (fracture). *Invest Radiol* 1985;20:498–503.
20. Nutton RW, Fitzgerald RH, Kelly PJ. Early dynamic bone imaging as an indicator of osseous blood flow and factors affecting the uptake of Tc-99m hydroxymethylene diphosphonate in healing bone. *J Bone Joint Surg* 1985; 67-A:763–770.
21. Smith MA, Jones EA, Strachan RK, et al. Prediction of fracture healing in the tibia by quantitative radionuclide imaging. *J Bone Joint Surg* 1987;69: 441–447.
22. Citrin DL, Bessent RG, McGinley E, Gordon D. Dynamic studies with Tc-99m-HEDP in normal subjects and in patients with bone tumors. *J Nucl Med* 1975;16:886–890.
23. Israel O, Front D, Frenkel A, Kleinhaus U. 24-hour/4-hour ratio of technetium-99m methylene diphosphonate uptake in patients with bone metastases and degenerative bone changes. *J Nucl Med* 1985;26:237–240.
24. Castronovo FP Jr., Kenneth A, McKusick KM, Strauss HW. The 4h/24h Tc-99m-MDP whole body retention: a new index of bone pathology. *Nucl Med Biol* 1986;13:599–602.
25. Alazraki N, Dries D, Datz F, Lawrence P, Greenberg E, Taylor A Jr. Value of 24-hour image (four-phase bone scan) in assessing osteomyelitis in patients with peripheral vascular disease. *J Nucl Med* 1985;26:711–717.
26. Arnold JS. Mechanisms of fixation of bone imaging radiopharmaceuticals. In: Billinghurst MW, Colombetti LG, eds. *Studies of cellular function using radiotracers*. Boca Raton, Florida: CRC Press Inc.; 1982;115–144, Band 5.
27. Sagar VV, Piccone JM, Charkes ND. Studies of skeletal tracer kinetics: III. Technetium-99m-(Sn) methylene diphosphonate uptake in the canine tibia as a function of blood flow. *J Nucl Med* 1979;20:1257–1261.
28. Rhinelander FW. The normal microcirculation of diaphyseal cortex and its response to fracture. *J Bone and Joint Surg* 1968;50-A:784–800.
29. Rhinelander FW, Baragry RA. Microangiography in bone healing. I. Undisplaced closed fractures. *J Bone and Joint Surg* 1962;44-A:1273–1298.
30. Huittinen V-M, Slätis P. Postmortem angiography and dissection of the hypogastric artery in pelvic fractures. *Surgery* 1973;73:454–462.
31. Matin P. The appearance of bone scans following fractures, including immediate and long-term studies. *J Nucl Med* 1979;20:1227–1231.
32. Nutton RW, Pinder IM, Williams D. Detection of sacroiliac injury by bone

scanning in fractures of the pelvis and its clinical significance. *Injury* 1981; 13:473–477.
33. McAfee PC, Yuan HA, Fredrickson BE, Lubicky JP. The value of computed tomography in thoracolumbar fractures. *J of Bone and Joint Surg* 1983;65-A:461–473.
34. Slavin JD, Mathews J, Spencer RP. Bone imaging in the diagnosis of fractures of the femur and pelvis in the sixth to tenth decades. *Clin Nucl Med* 1986;11:328–330.
35. Gertzbein SD, Chenoweth DR. Occult injuries of the pelvic ring. *Clin Orthop* 1977;128:202–207.

CORRECTION

The following table originally appeared on page 898 of "Plasma D-Dimer: A Useful Tool for Evaluating Suspected Pulmonary Embolus," Harrison et al., *J Nucl Med* 1993;34:896–898. The values in boldface type in the Spec and PPU columns have been corrected.

TABLE 3
V̇/Q̇ Results Versus D-D Results

		PAG+		PAG−					
	No. PAG	D-D+	D-D−	D-D+	D-D−	Sens	Spec	PPV	NPV
Low probability	21	4	0	5	12	1.00	**0.71**	**0.44**	1.00
Indeterminate	37	8	1	13	15	0.89	0.54	0.38	0.94
High probability	5	3	0	1	1	1.00	**0.50**	**0.75**	1.00
Total	63	15	1	19	28	0.94	0.59	0.44	0.97